*Essential Readings in Light Metals: Electrode Technology for Aluminum Production.*
Edited by Alan Tomsett and John Johnson.



# CARBON CATHODE CORROSION BY ALUMINIUM CARBIDE FORMATION IN CRYOLITIC MELTS

Xianan Liao and Harald A. Øye

Institute of Inorganic Chemistry
Norwegian University of Science and Technology
N-7034 Trondheim, Norway

## ABSTRACT

The carbon cathode corrosion by $Al_4C_3$ formation is electrochemical in nature. The corrosion in the presence of aluminium and a cryolitic melt without an externally applied current is galvanic; little corrosion occurs in an alumina-saturated acidic melt without short-circuit between the carbon sample (cathode) and the aluminium (anode). When an external current is applied, the corrosion is electrolytic and is one of the parallel cell reactions. Solid $Al_4C_3$ is formed electrochemically and it may subsequently dissolve chemically in the melt. Addition of $Al_4C_3$ reduces the galvanic corrosion due to its suppression of carbide dissolution and increased ohmic resistance. In the case of electrolytic corrosion, carbide addition was found to increase corrosion at a current density less than 0.2 A/cm$^2$, has little influence at a current density about 0.4 A/cm$^2$ and reduces corrosion at a current density greater than 0.6 A/cm$^2$.

## 1. INTRODUCTION

One of the two major mechanisms of carbon cathode wear is aluminium carbide formation and subsequent removal. This mechanism is referred to as corrosion or electrochemical (galvanic or electrolytic) corrosion in the present paper, since it is electrochemical in nature. The other mechanism is by detachment of particles and is referred to as abrasion or physical abrasion, because it is mainly caused by friction between the carbon cathode and solid alumina particles. The term erosion is frequently used in the literature when the carbon cathode wear is concerned, but it is an inaccurate word since in the terminology of tribology, erosion is defined as physical removal of material by impingement of particles or a liquid.

When there is no externally applied current (without electrolysis), the corrosion is driven by the potential difference between carbon and aluminium, the more noble carbon acting as a cathode undergoing reduction, and the more active aluminium acting as the anode undergoing oxidation. When an external current is applied, the corrosion is usually one of the parallel cell reactions.

The cathodic reaction is the same for galvanic and electrolytic corrosion:

$$3C\ (\text{cathode}) + 4AlF_3\ (\text{diss}) + 12e^- = Al_4C_3\ (s) + 12F^-\ (\text{diss}) \quad (1)$$

The anodic and corrosion reactions are different:

- Galvanic, e.g. in the presence of a cryolitic melt and aluminium or in aluminium alone:

$$\text{Anodic:}\quad 4Al\ (l) + 12F^-\ (\text{diss}) = 4AlF_3\ (\text{diss}) + 12e^- \quad (2)$$

$$\text{Corrosion:}\quad 3C\ (\text{cathode}) + 4\ Al\ (l) = Al_4C_3\ (s) \quad (3)$$

- Electrolytic, e.g. in aluminium electrolysis. According to Ødegård et al. [1] $Al_4C_3$ dissolves in a cryolitic melt according to the equilibrium:

$$Al_4C_3\ (s) + 5AlF_3\ (\text{diss}) + 9F^-\ (\text{diss}) = 3Al_3CF_8^{3-}\ (\text{diss}) \quad (4)$$

In electrolysis of a cryolitic melt with $Al_4C_3$ dissolved, $Al_3CF_8^{3-}$ is transported to the anode and is oxidized there[1, 2]:

$3Al_3CF_8^{3-}$ (diss) + $3F^-$ (diss) = 3C (anode) + $9AlF_3$ (diss) + $12e^-$ (5) *)

Adding Reactions (1), (4) and (5) together gives:

C (cathode) = C (anode) (6)

Since the corrosion is electrochemical in nature, it is important to use electrochemical principles to analyze the corrosion process. Factors affecting electrochemical corrosion include:

- Electrode potential, the data will indicate whether or not corrosion can occur.

Galvanic: The electrode potential can be calculated from the standard Gibbs energy of formation of $Al_4C_3$, e.g. -146 kJ at 980 °C [3]. The standard voltage of Reaction (3) is then 0.126 V. The galvanic corrosion is therefore thermodynamically favoured.

Electrolytic: The electrode potential will depend on the current applied.

- Polarisation, including concentration polarisation, reaction polarisation and resistance polarisation. Polarisation and other reaction kinetics control how fast corrosion can take place.
- Protective film characteristics, the solid reaction product $Al_4C_3$ may be present as a diffusion barrier, it may also provide a galvanic couple that increases the corrosion rate of active areas.
- Mass transport, including migration, diffusion and convection. An upper limit for the possible corrosion rate may be set by the availability of a reactant such as $Al^{3+}$.
- Melt environment, included in this group of factors are the melt temperature, volume and flow rate.
- Melt properties, depending on composition, because liquidus temperature, carbide solubility, viscosity and surface tension vary from melt to melt.
- Material properties, including graphitization degree, apparent density and porosity.
- Geometry, the shape and arrangement of electrodes, the area ratio between the anode and cathode may be also important.

Thus, electrochemical corrosion is a complex form of corrosion involving many factors.

## 2. EXPERIMENTAL

A similar set-up (Figure 1), sampling, wear rate measurement and experimental procedure as in reference [4] were used. The melt composition and some estimated properties are given in Table 1.

Table I. Composition and properties of an alumina-saturated cryolite-based melt with 5 wt% $CaF_2$ at 980 °C [1,5,6]

| CR | $S_A$ | $S_C$ | $S_m$ | $d_m$ | $t_{liq}$ | η | σ |
|---|---|---|---|---|---|---|---|
| 2.2 | 9.05 | 1.18 | 0.043 | 2.050 | 932 | 2.47 | 100 |

*) Under normal electrolysis conditions the oxidation of the dissolved carbide by the anode gas is probably the main oxidation mechanism.

CR: cryolite ratio: mol NaF/mol $AlF_3$,
$S_A$: solubility of alumina in the melt, wt%,
$S_C$: solubility of $Al_4C_3$, wt%,
$S_m$: solubility of aluminium, wt%,
$d_m$: density of the melt saturated with alumina, g/cm$^3$,
$t_{liq}$: liquidus temperature, °C,
η: viscosity of the melt saturated with alumina, mPa·s,
σ: surface tension of the melt saturated with alumina, mN/m.

In addition, the aluminium density is taken as 2.294 g/cm$^3$[5].

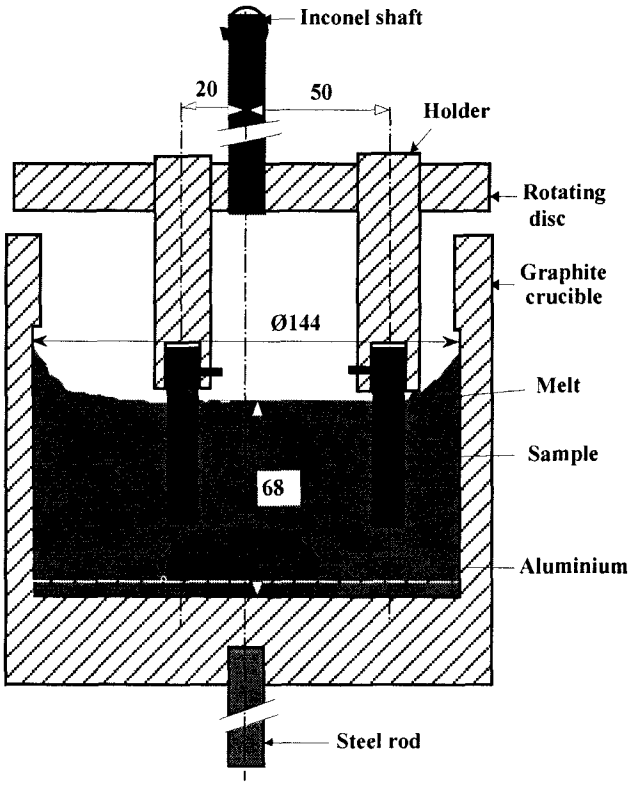


Figure 1: Set-up for galvanic corrosion study in the presence of a cryolitic melt and aluminium, dimensions are in mm. The rotating disc has one holder with a rotational radius of 50 mm and one holder with a rotational radius of 20 mm. The white broken line indicates the theoretical metal height (5 mm). The actual metal surface was curved as shown due to poor wetting between the metal and graphite. The distance between the sample and the bottom of the crucible was 30 mm.

The metal height ($H_M$) is defined as the hypothetical height in the crucible by assuming a flat metal surface. The sample-crucible bottom distance ($D_{S-C}$) is the distance between the sample and the inner bottom of the crucible. The 50 mm holder refers to the holder with a rotationa radius of 50 mm, and the 20 mm holder refers to the holder with a rotational radius of 20 mm.

The experimental conditions for the galvanic corrosion study and for the electrolytic corrosion study are the following:

For galvanic corrosion study: The total height of the melt and aluminium was 68 mm with or without $Al_4C_3$ (60 g) addition.

Three different metal levels: 5, 10 and 30 mm (assuming a flat surface) were used. For example, if the metal level was 10 mm, the system consisted of 1940 g melt and 375 g aluminium. The melt can dissolve 22.8 g $Al_4C_3$ [6], and the amount of carbide in excess of the solubility was 37.1 g for the experiments with carbide addition. Two samples were used for each experiment, one was connected to the holder with a rotational radius of 50 mm, and the other to the holder with a rotational radius of 20 mm (Figure 1).

For electrolytic corrosion study: The amount of melt was 2037 g (61 mm high in the crucible) plus 0 or 63 g $Al_4C_3$. The distance between the sample bottom and the crucible bottom was kept at about 35 mm. One sample was used for each experiment.

Because the graphite crucible was not lined with an inert material, it was expected to be subject to galvanic corrosion like the sample in the galvanic corrosion study. In order that the melt without carbide addition was not saturated with carbide in the whole experimental run, the test time was limited to one hour, if not otherwise specified, for experiments with rotating samples, i.e., two hours shorter than that in Reference [4]. For experiments with stationary samples, three hours of test time were used. In the second system the crucible served as anode and would not be consumed by carbide formation; the test time was usually three hours.

A new melt without carbide addition was used twice, it was then crushed and mixed with carbide powder. In order to ensure that the melt was saturated with $Al_4C_3$ in the experiments with carbide addition, the temperature was raised to 1020 °C and held there for one hour, then reduced to 980 °C and allowed to stabilize before the experiment was started.

The corrosion is expressed as volume loss ($mm^3$) or wear depth (mm) of the sample. The wear rate ($W_R$) is expressed as volume loss per hour ($mm^3/h$) or wear depth per year (cm/year). They are related by the following equation:

$$W_R \text{ (cm/year)} = 8.76\ W_R \text{ (mm}^3\text{/h)} / A_S \qquad (7)$$

$A_S$: The immersed surface area of the sample, $cm^2$. $A_S$ of one sample was usually 14.9 $cm^2$ for experiments in the galvanic corrosion study and 10.2 $cm^2$ for experiments in the electrolytic corrosion study.

## 3. RESULTS AND DISCUSSION

### 1. Galvanic corrosion

Figure 2 shows the influence of the metal height and the sample-crucible distance on the corrosion. The metal height of 10 mm gave the largest corrosion in both sample-crucible distances used. It was observed that when the metal height was 30 mm, the metal-melt interface could be seen on the sample since the interface had the largest corrosion, and that the part of the sample which extended into metal pool was only corroded slightly. When the sample was not extended into the metal pool (Experiments 2 and 5), the corrosion was very small and was within the experimental uncertainty. In Experiment 6 the sample connected in the 20 mm holder probably touched the curved metal surface since its corrosion was significantly greater than that of the sample connected in the 50 mm holder. The technical implication is that the exposed carbon sidewall in an aluminium electrolysis cell will be corroded quickly because the exposed sidewall, metal pad and melt constitute a short-circuit galvanic cell.

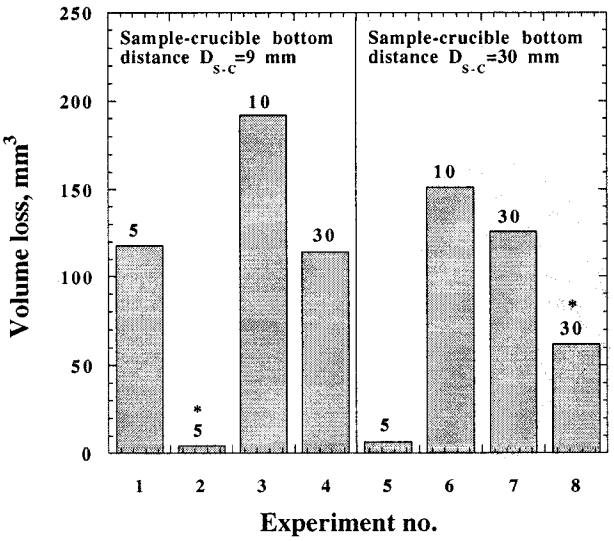


Figure 2: Volume loss of CS graphite in the mixture of a cryolitic melt and aluminium. Numbers on top of the bars indicate the metal heights. The volume loss is the sum of the two samples in the same experiment. Temperature, $t$=980 °C, velocity, $V$=0, test time=3 hours.
* Experiments with aluminium carbide addition.

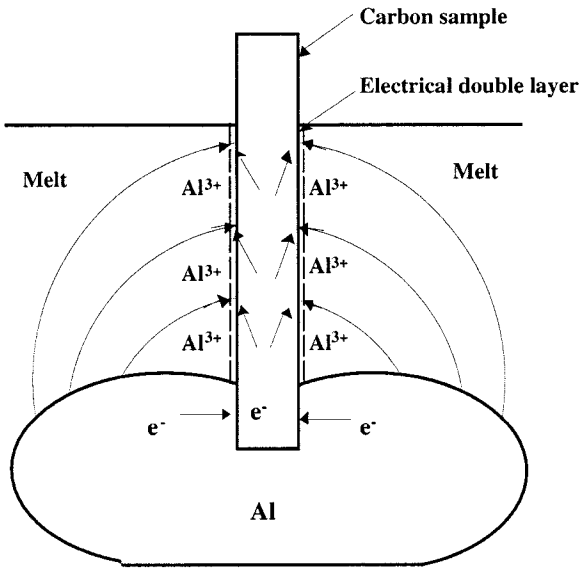


Figure 3: Current pathways in an internally short-circuited Al/carbon galvanic cell with a cryolitic melt as the ionic conductor, assuming the corrosion current is symmetric on both sides of the sample.

The corrosion mechanism can be analysed with help of Figure 3: When the sample is submerged into the metal pool through the melt, the system is virtually an internally short-circuited galvanic cell. The resistance polarisation increases from the carbon-melt-metal interface to the carbon-melt interface at the top surface of the melt. Electrons flow from the metal to the carbon and $Al^{3+}$ ions are transported to the electrical double layer on the cathode. The current in the melt is mainly carried by $Na^+$ ions from the metal side to the carbon side. In the electrical double layer on the anode, the metal oxidizes and dissolves into the melt. In the electrical double layer on the cathode the reduction reaction (Reaction 1) takes place on the carbon side and solid $Al_4C_3$ is formed. Significant corrosion which occurred in Experiment 8 in Figure 2, and Experiments 1, 3 and 5 in Figure 4 strongly supports the idea that solid $Al_4C_3$ is electrochemically formed because dissolved aluminium carbide cannot be formed in the carbide-saturated melt. The implication is that formation of $Al_4C_3$ is controlled by kinetical factors. According to Reaction (1), formation of dissolved carbide is thermodynamically favoured due to the reduced activity, but the real process is probably much more complicated than that indicated by Reaction (1). the kinetical factors are probably more important.

The corrosion was fairly even above the carbon-melt-metal interface, with the interface undergoing the largest corrosion because the resistance polarisation was the lowest and the corrosion current the highest. On the other hand the corrosion was much less intensive in the metal pool, probably due to the fact that the melt supply at the aluminium/carbon interface is limited. The solid carbide can dissolve chemically into an unsaturated melt and this was probably one of the main reasons why greater corrosion occurred in the experiments without carbide addition. Another main reason is that the resistivity of the melt without carbide addition is significantly lower than that of the melt with carbide addition [7], the corrosion current is hence higher in the melt without carbide addition. The very small corrosion in Experiment 2 (Figure 2) was probably because the sample did not touch the metal surface, since the excess carbide powder (≥37.1 g) settled down on the crucible bottom and the metal was found to be divided into several small round pieces after cooling, probably due to strong surface tension between the metal and the carbide powder. The metal height was hence lowered since it took more bottom space.

Figure 4 shows the volume loss as a function of carbide addition, test time and rotating speed. The wear increases with rotating speed and test time, and decreases with carbide concentration. In the experiments with carbide addition, dimension measurements showed that the maximum wear depth was about 0.02 mm for Experiments 1 and 3 and about 0.06 mm for Experiment 5. The metal became small spheres with a diameter of 2-5 mm after Experiment 5, indicating that there had been a strong interface reaction between the metal and the carbide powder caused by surface tension. The wetting between aluminium and $Al_4C_3$ was probably very poor.

The results that galvanic corrosion occurred in the carbide saturated cryolitic melt is consistent with our earlier study [4] where significant wear was observed in the melt with 3 wt% carbide addition. The observations that the wear rate decreased with time and finally became nearly zero [4, 8] were probably due to the formation of a solid $Al_4C_3$ film which acted as a diffusion barrier. If new samples were introduced, smaller but still significant wear would occur. This means that whenever a cryolitic melt, aluminium and carbon are in contact, solid $Al_4C_3$ will be formed on the carbon surface no matter whether the melt is saturated with carbide or not. However, the removal of $Al_4C_3$ from the surface by chemical dissolution will be stopped in the carbide saturated melt and hence the wear is reduced.

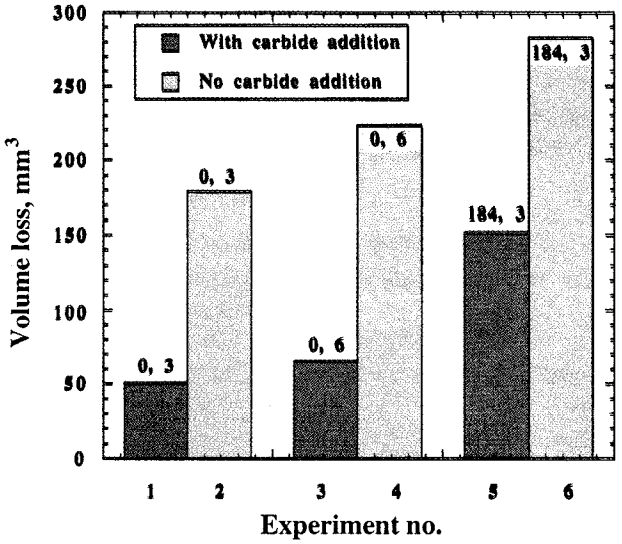


Figure 4: Volume loss of CS graphite in the presence of a cryolitic melt and aluminium. The volume loss is the sum of the two samples in the same experiment. The metal level was 10 mm. The sample-crucible distance was 9 mm for stationary samples and 20 mm for rotating samples. Numbers on top of the bars indicate the rotating speed (rpm) and the test time (hour), respectively. $t$=980 °C.

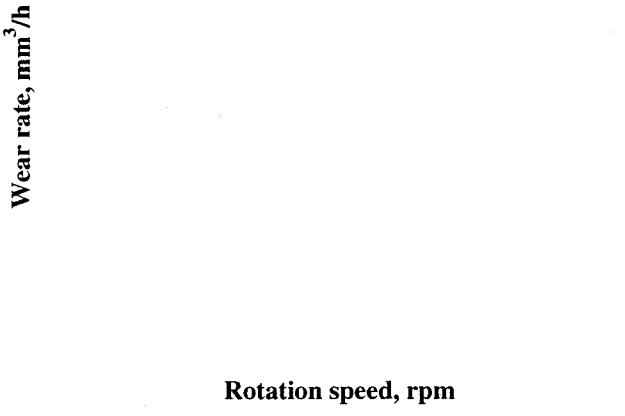


Figure 5: Wear rate of CS graphite as a function of rotation speed in the cryolitic melt and aluminium without electrolysis. The metal height was 5 mm. Numbers in the first column denote the sample-crucible bottom distance, and numbers in

the second column denote the holder used. $t$=980 °C, test time=1 hour for rotating samples and 3 hours for static samples.

Figure 5 shows the wear rate, expressed as volume loss in $mm^3$ per hour, of CS graphite as a function of rotation speed in the mixture of the cryolitic melt and aluminium. The sample-crucible bottom distance was varied. Since the metal level was low (5 mm), there should hardly be short-circuit between the sample and the metal pool when the sample-crucible bottom distance was 20 mm and 35 mm and the sample was stationary.

Three characteristics can be seen from Figure 5:

a) The wear rate increased when the sample-metal distance was reduced, probably because the mass transfer and the possibility of forming short-circuit galvanic cells increased when the distance was reduced. Since the metal solubility in the melt is very small, the corrosion rate was very small without short-circuit.

b) The wear rate increased with the rotation speed. This is the expected trends for the mass transfer and the possibility of forming short-circuited galvanic cells increases when the rotation speed is increased.

c) The wear rate of the sample in the 20 mm holder is often greater than that of the sample in the 50 mm holder at low rotation speeds. This was probably because the metal surface was not flat but curved and the sample in the 20 mm holder was closer to the metal than the sample in the 50 mm holder. The possibility of short-circuit for the sample in the 20 mm holder was hence larger.

2. Electrolytic corrosion

The wear rates of CS graphite in alumina-saturated cryolitic melts with or without $Al_4C_3$ addition are shown in Figure 6.

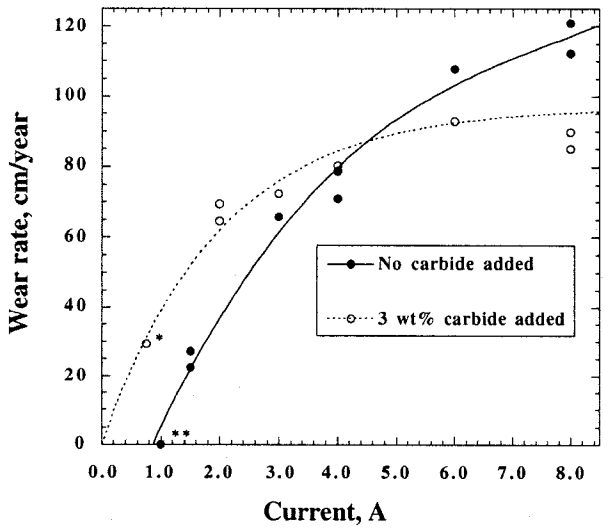


Figure 6. Wear rate of CS graphite as a function of current. One sample was used for each experiment, $V$=0.55-0.6 m/s, $t$=980 °C, test time=3 hours, no aluminium added.
* Only 22 g $Al_4C_3$ (≈1 wt%) was added. ** Three experiments were performed and none gave wear.
The cathodic current density CCD = 0.073–0.837 $A/cm^2$.

It is seen from Figure 6 that the wear rate in the melt with carbide addition is:

- Larger than that in the melt without carbide addition at a current of 2 A or less (current density ≤ 0.2 $A/cm^2$).
- Similar to that in the melt without carbide addition in the vicinity of 4 A (current density ≈ 0.4 $A/cm^2$).
- Smaller than that in the melt without carbide addition at a current of 6 A or more (current density ≥ 0.6 $A/cm^2$).

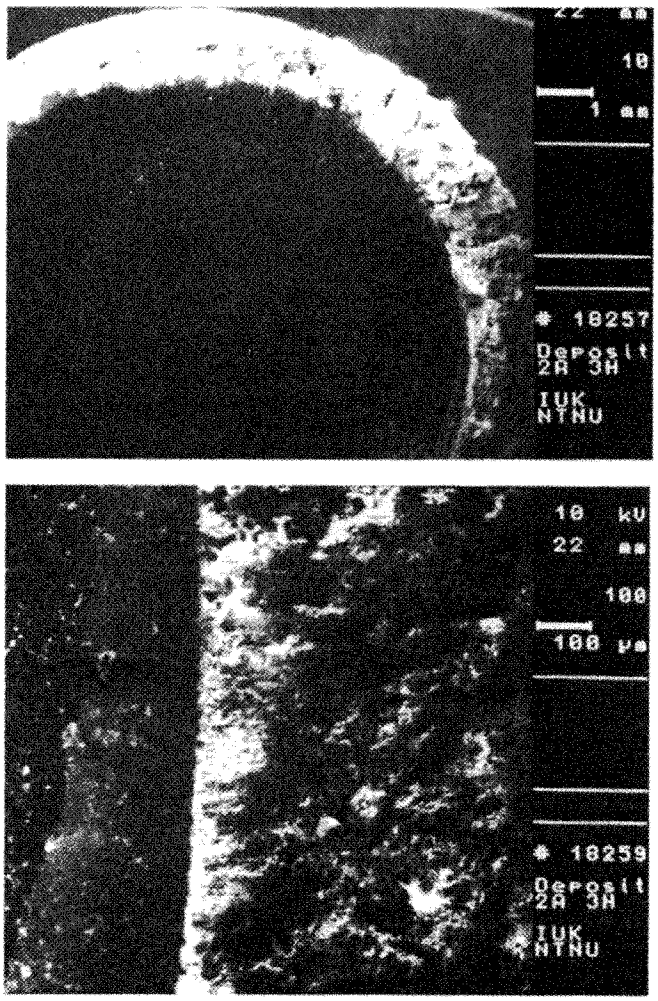


Figure 7. SEM pictures on the deposit on the CS graphite sample. The sample had been electrolysed at 2 A for three hours. Top: 10 ×, bottom: 100 ×.

Another important characteristic in Figure 6 is that no wear occurred in the melt without carbide addition at 1 A. After only 22 g (about 1 wt%) carbide was added to that used melt, significant wear occurred at only 0.75 A. The possible reasons

why wear can occur at a lower current in the melt with carbide addition are:

1. It has been observed that some deposit (Figure 7) has been formed on the sample surface after electrolysis with 2 A or less in the melt without carbide addition, the deposit is probably rich in alumina and hinders the cathode from dissolving. Little deposit is observed on the sample surface electrolysed in the melt with carbide addition. As for the mechanism for the deposit formation, it is possible that there exist fine undissolved alumina particles in the melt. These particles and melt may form a lyophilic colloid because of the strong affinity between them. The alumina content difference between the top and the bottom of the crucible was small [9], this was an indication of formation of the lyophilic colloid. It is known that a cryolitic melt does not wet carbon, addition of aluminium to the melt and/or cathodic polarisation of the carbon improve the wetting, thus the alumina colloid can stick onto the carbon and form a deposit on it. Carbide addition (including fine carbon dust) may affect the stability of the alumina colloid, or affect the interfacial properties between the cathode and the alumina particles so that an adhesive deposit cannot be formed.

2. Addition of $Al_4C_3$ lowers the liquidus temperature and improves the wetting between the melt and the carbon cathode. This helps to clean the sample surface and probably to increase the carbide current efficiency.

3. The cell voltage is lowered by more than one volt with carbide addition. This is because aluminium-producing cell reactions are different in the melt without carbide addition than in the melt with carbide addition:

Without carbide addition:

$$Al_2O_3\ (s) + 3C\ (s) = 2Al\ (l) + 3CO\ (g) \qquad (8)$$

CO is expected to form because of the low current density at the anode. The standard voltage for Reaction (8) is close to 1.1 V.

With carbide addition:

$$Al_4C_3\ (s) = 3C\ (s) + 4Al\ (l) \qquad (9)$$

The standard voltage for Reaction (9) is 0.126 V at 980 $^0$C [3], or nearly 1 volt less than that of Reaction (8). In addition the anodic overvoltage for Reaction (8) is probably larger than that of Reaction (9). Because the area of the anode (crucible) is much larger than that of the cathode (sample), an electrolysis current of 1 A may not give high enough polarization for CO evolution at the anode, hence aluminium cannot be produced at the cathode either. However, Reaction (9) can take place at a lower polarisation and aluminium can be produced provided the melt contains dissolved carbide. Aluminium can improve the wetting between a cryolitic melt and carbon, and this is perhaps important for the corrosion.

Finally it seems from Figure 6 that there exist maximum wear rates in the melt without carbide addition and the melt with carbide addition. This would mean that there exist corresponding limiting corrosion current densities in both cases. We can assume that some steady-state $Al^{3+}$ concentration gradient between the cathode surface and the bulk melt is established. The surface concentration is given by the following equation:

$$C^S = C^B - \frac{i\delta}{DZF} \qquad (10)$$

or:

$$i = ZFD\frac{(C^B - C^S)}{\delta} \qquad (11)$$

where $C^S$ is the $Al^{3+}$ concentration at the cathode surface, $C^B$ is the $Al^{3+}$ concentration in the bulk melt, $i$ is the externally applied cathodic current density for carbide formation, $\delta$ the diffusion layer thickness, $D$ the diffusion coefficient, $Z$ equals 4 here and $F$ is the Faraday constant.

The limiting current density $i_L$ for carbide formation at the cathode is given by the following equation:

$$i_L = \frac{ZFDC^B}{\delta} \qquad (12)$$

Since $C^B$ is quite large, especially in acidic melts, the limiting corrosion current density would be very large too if $Al^{3+}$ is not blocked at the cathode surface. The mechanism for the limiting current phenomenon is probably that a solid $Al_4C_3$ film is formed on the sample surface and this film presents a diffusion barrier to $Al^{3+}$. The carbide film probably consists of loosely-packed particles and its removal from the cathode surface can be chemical dissolution and physical detachment. The removal of the carbide film is expected to be slower in the carbide-saturated melt than in the melt without carbide addition since the carbide cannot dissolve into a saturated melt. The limiting corrosion current density in the melt with carbide addition is therefore lower than that in the melt without carbide addition.

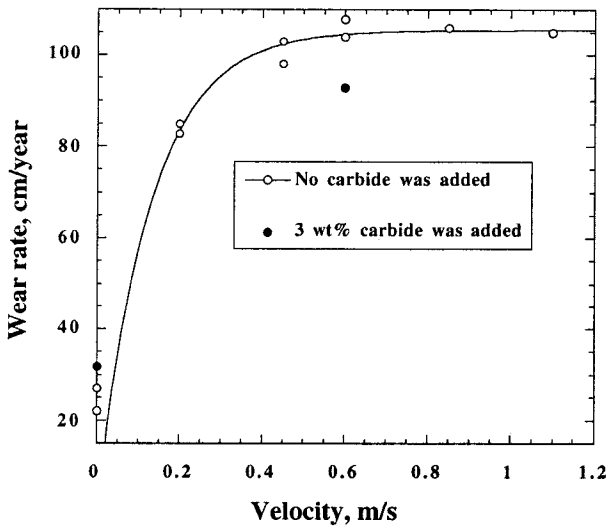


Figure 8. Wear rate of CS graphite as a function of velocity. The electrolysis current=6 A (CCD≈0.6 A/cm$^2$), $t$=980 °C, test time=3 hours, no aluminium added.

Figure 8 shows that the wear rate increases rapidly when the velocity is increased from 0 to about 0.6 m/s, indicating that the wear process is controlled by mass transfer in this velocity regime. Further increase in velocity seems to have little effect on the wear rate, so that the wear process may be controlled by chemical reaction in the electrochemical double layer.

### 3. Corrosion image

Carbon samples undergoing corrosion (galvanic or electrolytic) look dull. This is contrary to the samples undergoing abrasion, which look shiny [10]. The corrosion is fairly even macroscopically over the immersed part of the sample. However, the binder phase seem to be corroded preferentially, and the protruding grains can be clearly seen (Figure 9).

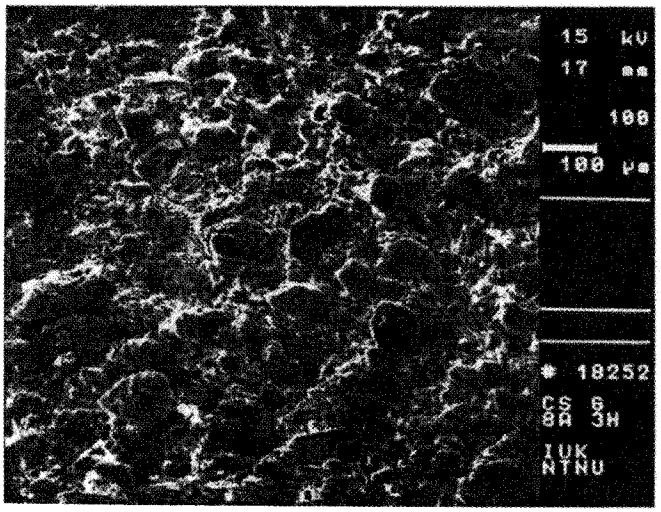


Figure 9. SEM picture of an electrolysed CS graphite sample.

## 4. CONCLUSIONS

1. The corrosion of carbon in the presence of a cryolitic melt and aluminium is galvanic in nature. Solid $Al_4C_3$ is formed electrochemically and it may subsequently dissolve chemically in the melt.

2. The wear rate of graphite during electrolysis of the melt increases with rotational velocity up to about 0.6 m/s. After that the velocity has little effect and the wear process is probably controlled by the electrochemical step.

3. Addition of $Al_4C_3$ into the melt increases the wear at a current density less than 0.2 A/cm$^2$, and decreases the wear at a current density greater than 0.6 A/cm$^2$.

4. At the industrial current densities of about 0.8 A/cm$^2$, the wear rate was found to be reduced by about 25% by addition of aluminium carbide grains.

*Acknowledgment*: S. Jarek, H. Kvande, J. Thonstad, B. Welch and M. Sørlie are thanked for very useful comments to the manuscript. Financial support from The Research Council of Norway and the Norwegian aluminium industry is gratefully acknowledged.

## REFERENCES

1. R. Ødegård, Å. Sterten and J. Thonstad, "On the Solubility of Aluminium Carbide in Cryolitic Melts," Light Metals 1987, 295-302.
2. R. Ødegard, Å. Sterten and J. Thonstad, , "On the Solubility of Aluminium Carbide and Electrodeposition of Carbon in Cryolitic Melts," J. Electrochem. Soc., **134** (1987), 1088-1092.
3. W. L. Worrell, "Carbothermic Reduction of Alumina: A Thermodynamic Analysis," Can. Met. Quart. **4** (1965), 87-95.
4. X. Liao and H. A. Øye, "Physical and Chemical Wear of Carbon Cathode Materials", Light Metals 1998, 667-674.
5. K. Grjotheim and H. Kvande, Introduction to Aluminium Electrolysis (2nd edition, Aluminium-Verlag, Dusseldorf, 1993).
6. R. Ødegård, Å. Sterten and J. Thonstad, "On the Solubility of Aluminium in Cryolitic Melts", Metallurgical Transactions B , **19B** (1988), 449-457.
7. L. Wang, A. T. Tabereaux and N. E. Richards, "The Electrical Conductivity of Cryolite Melts Containing Aluminium Carbide", Light Metals 1994, 177-185.
8. P. A. Skjølsvik, J. Mittag and H. A. Øye, "Consumption of Cathode Materials due to $Al_4C_3$ Formation", Aluminium **67** (1991), 905-909.
9. X. Liao and H. A. Øye, "Increased Sodium Expansion in Cryolite-basd Alumina Slurries", Light Metals 1998, 659-666.
10. X. Liao and H. A. Øye, "Method for Determination of Abrasion Resistance of Carbon Cathode Materials at Room Temperature", Carbon, **34** (5), 1996, 649-661.